J. Phys. Earth, 34, 19–42, 1986

T-WAVE DURATION, MAGNITUDES AND SEISMIC MOMENT OF AN EARTHQUAKE—APPLICATION TO TSUNAMI WARNING

Emile A. OKAL* and Jacques TALANDIER**

**Department of Geological Sciences, Northwestern University, Evanston, Illinois 60201, U.S.A.*
***Laboratoire de Géophysique, Commissariat à l'Energie Atomique, Boite Postale 640, Papeete, Tahiti, French Polynesia*

(Received June 6, 1985; Revised November 16, 1985)

We present a study of the duration, Θ, of T wave trains propagating over teleseismic distances in the ocean, and recorded at island stations, in relation to the various magnitudes (m_b, M_s, M_w) of the parent earthquake. Theoretical models based on scaling laws predict relations of the form $\log_{10}\Theta = a + bM$, with the slope b equal to 1/3 at low magnitudes, but increasing to 1/2 (and eventually to 1) because of the effect of saturation of the magnitude scales. The investigation of an extensive dataset using records of more than 400 Pacific earthquakes shows a remarkable agreement with these theoretical slopes. In the case of truly large earthquakes ($M_w > 7$), such relations allow an estimation of the earthquake's seismic moment at ultra-long periods within 1 to 2 hr of the origin time, with important applications to efficient tsunami warning.

1. *Introduction*

The need for a reliable method to protect continental and island shores from the devastating effects of tsunamis is self-evident. Large tsunamis are generated by underwater seismic events, and most tsunami-warning procedures rely on some kind of interpretation of the seismic waves of the parent earthquake. In order to avoid the false alarms (e.g., Aleutian Islands, 30 March 1965) which strongly affect the credibility and the social impact of future warnings (see, for example, EATON *et al.* (1961) on the 1960 Chilean tsunami), it is desirable to assess quantitatively the tsunami danger from an earthquake. In doing so, one does not consider local factors, such as resonant effects of bays and harbors, which control the local deformation of a tsunami wave as it reaches shore, but rather concentrates on the potential that the earthquake has of generating a large tsunami on the high seas.

The question of the relation of the size of the parent earthquake to the observed tsunami has long been a challenge to seismologists. Pioneering studies (IIDA, 1970; WATANABE, 1970) based on the use of 20-s surface wave magnitudes M_s have not been totally successful, and KANAMORI (1972) and FUKAO (1979) have

focused on the so-called "tsunami earthquakes," whose tsunamis are much greater than expected from their M_s values (e.g., Nankaido, 1946; Aleutian, 1946; Sanriku, 1896; Kurile, 20 Oct. 1963; Nemuro-Oki, 10 June 1975). This is due in part to the saturation of M_s around 8.2, which has been explained in terms of scaling laws by GELLER (1976). In order to adequately describe the size of gigantic earthquakes, KANAMORI (1977) introduced the so-called "energy magnitude" M_w, supposedly measured at zero-frequency, and related to the seismic moment through:

$$M_w = (\log_{10} M_0 - 16.1)/1.5 \; . \tag{1}$$

Careful studies by KANAMORI (1972) and ABE (1973) have suggested that the seismic moment M_0 of the earthquake, representative of the source behavior at zero-frequency, was indeed the fundamental factor in tsunami excitation. This is due to the fact that the energy of tsunami waves is concentrated mostly in the ultra-long period part of the seismic spectrum, typically around 1,000 s. This result, explained theoretically by BEN-MENAHEM and ROSENMAN (1972) and by WARD (1980), was confirmed in an extensive review of tsunamigenic earthquakes (ABE, 1979), which proved that KANAMORI's (1977) M_w correctly predicts tsunami amplitudes. A fundamental step toward making tsunami warning more precise and reliable is thus to devise a method of measuring M_0 or M_w in real time.

In practice, and because no earthquake greater than $M_w = 9.5$ has ever been recorded, M_w is measured using ultra-long period surface waves ($T \simeq 300$ s), a procedure reviewed by KANAMORI and GIVEN (1983). In order to eliminate the influence of such parameters as radiation pattern and directivity, this procedure requires the compilation of data from many observatories around the world. Additionally, present-day digital instruments, such as those of the IDA network, saturate or exhibit strong non-linearity at amplitudes characteristic of the first passage of surface waves from gigantic events (e.g., AGNEW *et al.*, 1976), and thus only the subsequent surface wave trains can be processed. Thus, even in the age of instant satellite telecommunications, at least four or five hours are needed to obtain an estimate of the ultra-long period magnitude M_w. On the other hand, a faster estimate might be needed for the purpose of tsunami warning.

WARD (1980) has proposed to use body-wave inversion techniques to retrieve the moment tensor of the earthquake in quasi-real time from SRO-type digital data. However, such measurements are not taken at the ultra-long periods characteristic of tsunami excitation (for which the body-wave concept breaks down), and it is doubtful that this technique would correctly describe the so-called "tsunami earthquakes."

EWING *et al.* (1950) were the first to propose the use of T waves, travelling in the SOFAR low-velocity channel of the oceanic column, in tsunami warning programs. TALANDIER (1966) applied this method using the French Polynesia

Seismic Network (Réseau Sismique Polynésien [RSP]),* and later identified the duration of the T wave train as the crucial parameter for the identification of tsunamigenic earthquakes (TALANDIER, 1972). Note that the amplitude of the T waves, locally controlled by topographic features on a scale of 1 km or less, is not directly related to the size of the potential tsunami. This point was dramatically illustrated in the June 22, 1977 Tonga earthquake, whose T waves had very large amplitudes, and were actually felt in Tahiti, 2,800 km away from the epicenter, but which generated only a modest tsunami (TALANDIER and OKAL, 1979).

The purpose of this paper is to describe the theoretical foundations of this empirical method, and to examine some of the problems associated with it, using an extensive database of T wave records at Pacific island stations, following major earthquakes in the Pacific Ocean.

2. *Theory*

The relationship existing between the moment of an earthquake and the duration of T waves observed at teleseismic distances stems from the fact that both parameters are controlled by the length of rupture L during the faulting. For most interplate events, scaling laws (KANAMORI and ANDERSON, 1975; GELLER, 1976) have been shown to exist over a wide range of earthquake sizes, and the proportionality between M_0 and L^3 has been explained theoretically and confirmed by observations. Due to the finiteness of rupture velocities, the duration of rupture itself is roughly proportional to L. As we will show, for large earthquakes, this becomes the preponderant factor governing the duration of the T wave train. The use of duration is indeed current practice in body wave studies of regional seismicity (HERRMANN, 1975; SUTEAU and WHITCOMB, 1979).

The factors affecting the duration of the T wave train observed at a teleseismic station are in the natural order of the phenomena involved:

1. the rise time of the source;
2. the mechanism of generation of the T wave, including directivity effects;
3. dispersion of the T wave during acoustic propagation;
4. multipathing;
5. the mechanism of the conversion of the T wave back to a seismic wave at the island shore, and its propagation to the recording station.

They will now be discussed in a slightly different order.

2.1 *Rise time*

The rise time τ_r of an earthquake source can be defined as the time it takes for the slip Δu to physically take place at a given location. It is expected to grow

* Strictly speaking, T phases can only be recorded at sea by hydrophones; however, the seismic wave generated by their conversion at an island shore can be recorded by a seismometer on the island, and for simplicity we will call this a seismic record of the T wave. Problems involved at the acoustic-seismic conversion are discussed in Section 2.4.

with earthquake size, since individual pieces of rock cannot move with infinite velocity, and Δu itself grows linearly with L according to scaling laws (GELLER, 1976). However, since rise times have rarely been reported to exceed 10 s, we will see that this represents a negligible contribution to the duration of T waves for earthquakes having tsunamigenic potential. Much longer source processes, involving for example multiple events, are usually described in the context of a propagating rupture, since it is likely that they correspond to different asperities (LAY and KANAMORI, 1981), as will be discussed in Section 2.5.

2.2 Dispersion during propagation

Since T waves are trapped in a low-velocity channel, they correspond to a maximum of the Fermat integral (travel-time), and are expected to be dispersed as a result of wave-guide propagation. PORTER (1973) has investigated this dispersion on the basis of experimental results from underwater grenades in the Mediterranean. His results show that the maximum dispersion is about 1.9% in group velocity, or 2 s over 160 km. He was able to interpret the propagation of the T wave as resulting from multiple reflections between the top and the bottom of the oceanic column. In the Pacific Ocean, where the SOFAR channel is more pronounced (JOHNSON and NORRIS, 1968), CANSI (1981) has shown that propagation over very large distances is confined to the SOFAR channel, and that dispersion plays an insignificant role on the shape of the T wave train.

This is also confirmed by the data shown on Fig. 1, consisting of routine records, at Tiputa (TPT) and Rauvai (RUV), of the T waves generated during a seismic refraction campaign off the coast of Southern California in November 1981, and involving a succession of shots at 10-s intervals. TPT and RUV are located on the northern coast of the atoll of Rangiroa, in French Polynesia. Although the exact nature of the shots is not known, they are clearly an excellent approximation to a point source, both in time and space. The T wave travelled approximately 6,100 km to the atoll's slope, where it was converted to a seismic wave. Since the stations are installed about 200 m from the ocean shore, the distance travelled by the seismic wave was minimal. This layout thus eliminates most source and receiver effects, and the duration of the T wave train (about 2 or 3 s or less than 0.1% of the total travel time for the records shown on Fig. 1) represents the contribution of dispersion, multipathing and other path effects. In the case of large earthquakes, this contribution would clearly become negligible, given the precision of the measurement of T wave duration, as discussed in Section 3.3.

2.3 Multipathing

Multipathing not directly related to the propagation in the waveguide usually takes the form of later arrivals due to efficient reflection on seamounts and atolls. These effects have long been documented (e.g., NORTHROP, 1974); the travel-time differences involved can be much longer than the typical duration of recorded T

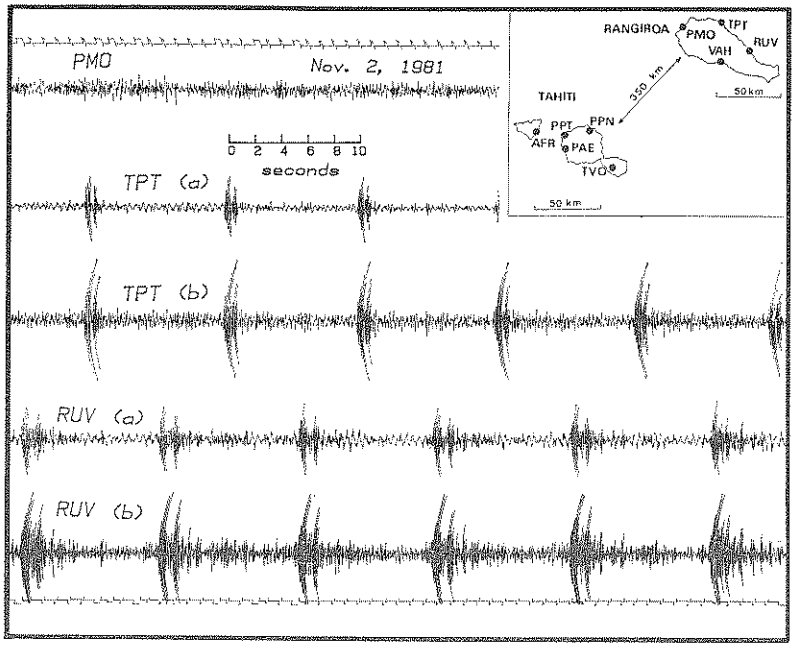

Fig. 1. T waves recorded at the Rangiroa, French Polynesia, subarray during a campaign of seismic refraction off the coast of California. The inset gives the geometry of the stations displayed. Channels (a) operate between 2 and 16 Hz, with a gain of 4×10^6 at 5 Hz; channels (b) between 3 and 16 Hz, with a gain of 8×10^6 at 5 Hz. Note the extremely short duration of the T wave, as well as the small multipathing, resulting in a second arrival whose time lag is station dependent.

wave trains; additionally, the amplitude of later arrivals is usually significantly lower than that of the first arrival, especially for large earthquakes.

2.4 Conversion at the receiving shore

The mechanism of conversion of a T wave back to seismic energy upon reaching a coastline is an extremely complex one. CANSI (1981, 1982) and CANSI and BETHOUX (1985) have shown that depending on the geometry of the coastlines, and the position of the seismic station inland, the shape of the resulting seismogram can vary greatly; in particular, in the case of continental stations located far inland, conversion can take place along a very long segment of coastline, and result in P_g, S_g and possibly L_g waves.* In the case of island stations, necessarily very close to the conversion slope, the problem is simplified and the propagation of the seismic wave becomes irrelevant, since it cannot contribute more than a few seconds to the length of the recorded wave train. This is illustrated in Fig. 1: a

* We use the conventional symbols P_g and S_g for crustal P and S phases; in the oceanic environment, propagation takes place in a basaltic layer and better (although less universal) symbols would be P_b and S_b.

second arrival is clearly present on all records, with a time lag of 0.6 s at TPT and 1.0 s at RUV. This suggests two conversion points along the slope; because of the proximity of the atoll stations to the shore line, this effect is minimal, but we should keep in mind that it could become important if the stations were located 100 km or more inland.

2.5 Source rupture and generation process of the T wave

That leaves the history of source rupture, and its influence on T wave generation, as the major contributor to the duration of their observed records on oceanic islands.

The finite rupture time, t_R, of an earthquake source is due to the fact that the initiation of rupture does not propagate immediately across the whole faulting area, but rather at a finite velocity v_R, usually found to be slightly less than the medium's shear velocity β (GELLER, 1976). As a result, a classic directivity effect is involved, with the duration Θ of T waves given by:

$$\Theta=(L/v_R)\left[1-\left(\frac{v_R}{c}\right)\cos\theta\right], \tag{2}$$

when observed at an azimuth θ from the direction of rupture propagation. Here, L is the length of the fault and $c\simeq 1{,}500$ m/s, the velocity of T waves.

This formula assumes, however, that the T wave is generated at the moving source, in the faulting area. This is a priori not the case, since the T wave can be generated only at the water-solid interface. Indeed, the mechanism by which T waves are generated at an epicenter remains obscure, since it is controlled by local topography on the scale of the wavelengths involved, typically $\lambda\simeq 500$ m, clearly beyond the precision of our present knowledge. In the simple case of Fig. 2(a) drawn for a fault propagating along a perfect ocean coastline, where the slope has no lateral heterogeneity, the travel time of the seismic wave (P or S) between the moving source and the T wave generation area remains a constant and this formula would apply. This situation would be approached by a major interplate event, such as the 1958 Alaska earthquake studied by BEN-MENAHEM and TOKSÖZ (1963).

A more representative case, however, would involve T waves generated at clearly preferential sites along the conversion slope. This is due in part to the fact that the trapping of seismic energy into the SOFAR channel requires an incidence angle of no more than 12 deg (with respect to the horizontal), and is greatly facilitated by a strongly dipping ocean floor (EWING *et al.*, 1950; TALANDIER, 1972). An example of extremely efficient conversion 40 km away from the epicenter was given by TALANDIER and OKAL (1979) following the intermediate depth Tonga earthquake of 1977. In this case, schematized in Fig. 2(b), and assuming P wave propagation at velocity α prior to the seismic-acoustic conversion, the following formula would apply:

$$\Theta=(L/v_R)\left[1-\frac{dv_R}{L\alpha}\left(\frac{1}{\cos\theta_1}-\frac{1}{\cos\theta_2}\right)\right]. \tag{3}$$

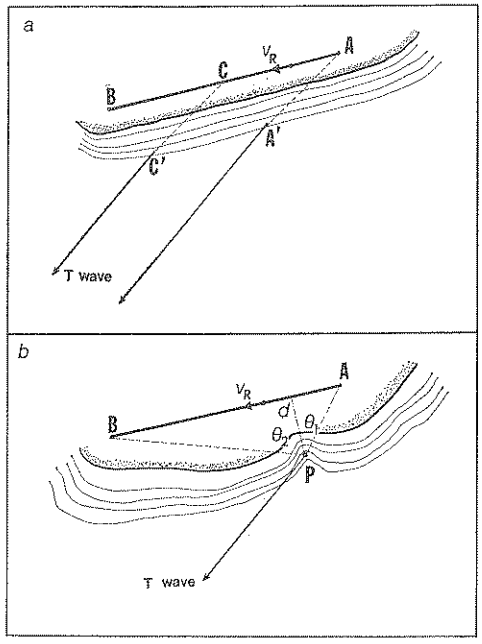

Fig. 2. Theoretical models of T wave generation for a rupture propagating from A to B at a rupture velocity v_R. (a) Case of a laterally homogeneous coastline and slope structure, for which the seismic-to-acoustic conversion takes place at each point C′ along the slope. In this case, the path AA′ or CC′ is a constant, and a classic directivity formula is obtained. (b) Case of a slope element P acting as a focusing point at which all seismic-to-acoustic conversion takes place. In this case, the travel-time of the T wave in the water is a constant, but the path of the seismic wave varies from d to BP. As mentioned in text, real-life situations are probably intermediate between these two extremes.

In a real life situation and for a very long rupture L, given the exact topography of the ocean floor in the vicinity of the source, the computation of the excitation of the T wave could be done by first computing the strong motion displacement field at each point of the ocean floor, and then considering these points as secondary sources in the formalism of Huygens' principle (e.g., SOMMERFELD, 1964). In practice however, it is probably easier to think of the generation of T waves as concentrated in a number of preferential areas comparable to that described above in (3). Conversion of energy from seismic to acoustic at other, less efficient, points along the slope will merely result in the coda of the T wave train, which is expected to be of lesser amplitude, and will not contribute to the most intense part of the observed wave train.

Comparison of formulae (2) and (3) suggests an average value

$$\Theta = C_{tR} = CL/v_R \tag{4}$$

for the effect of the source on the duration of the T wave train. Here, C is a geo-

metrical constant depending on the particular conditions at the generating slope, and whose value will be taken between 0.5 and 2. We then can use GELLER's (1976) relation between fault length and moment

$$M_0 = AL^3\Delta\sigma \ , \tag{5}$$

with $A=0.145=1.45\times10^{20}$ dyn-cm/(km$^3\times$bars). Substituting into (4), with average values of stress drop $\Delta\sigma=50$ bars and rupture velocity $v_R=3$ km/s, we obtain:

$$\log_{10}\Theta = \frac{1}{3}\log_{10} M_0 - 7.76\pm0.3 \ , \tag{6}$$

where Θ is in seconds, M_0 in dyn-cm, and the term ±0.3 represents the contribution of the unknown C in (4). The physical principles underlying this equation are the same as in HERRMANN (1975).

2.6 Relation with standard magnitude scales

The body- and surface-wave magnitudes m_b and M_s are the most commonly used estimates of an earthquake's size. Because of the finite dimension of earthquake sources, these various scales saturate, and we refer to GELLER (1976) for theoretical relations between m_b, M_s, and the seismic moment M_0. When combined with these expressions, Eq. (6) yields:

$$\log_{10}\Theta = 0.5M_w - 2.39\pm0.3 \quad \text{(all } M_w\text{'s)} \tag{7}$$

$$\log_{10}\Theta = M_s - 6.65\pm0.3 \quad (M_s<8.22) \tag{8a}$$

$$\log_{10}\Theta = \frac{1}{2}M_s - 2.59\pm0.3 \quad (M_s<8.12) \tag{8b}$$

$$\log_{10}\Theta = \frac{1}{3}M_s - 1.46\pm0.3 \quad (M_s<6.76) \tag{8c}$$

$$\log_{10}\Theta = m_b - 5.37\pm0.3 \quad (m_b<6) \tag{9a}$$

$$\log_{10}\Theta = \frac{1}{2}m_b - 2.60\pm0.3 \quad (m_b<5.55) \tag{9b}$$

$$\log_{10}\Theta = \frac{1}{3}m_b - 1.91\pm0.3 \quad (m_b<4.19) \ . \tag{9c}$$

In the next section, we use a dataset of several hundred Pacific earthquakes to investigate experimentally the relationship between Θ and the various magnitude scales.

3. *Observations*

Typical examples of records of T waves are presented on Figs. 3 and 4. It is immediately apparent that defining the "duration" of the wave train is not easy. In particular, for very large earthquakes and as discussed in Section 2.5, the process

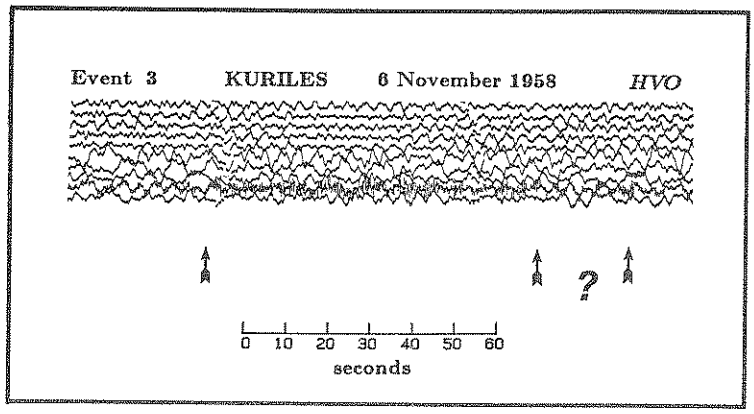

Fig. 3. Example of T wave record, for the 1958 Kuriles event at Hawaii Volcano Observatory (HVO). Note that the onset of the maximum of amplitude in the T wave train is easy to identify (left arrow), but that some uncertainty remains as to its end (right arrows). This constitutes a typical HVO record.

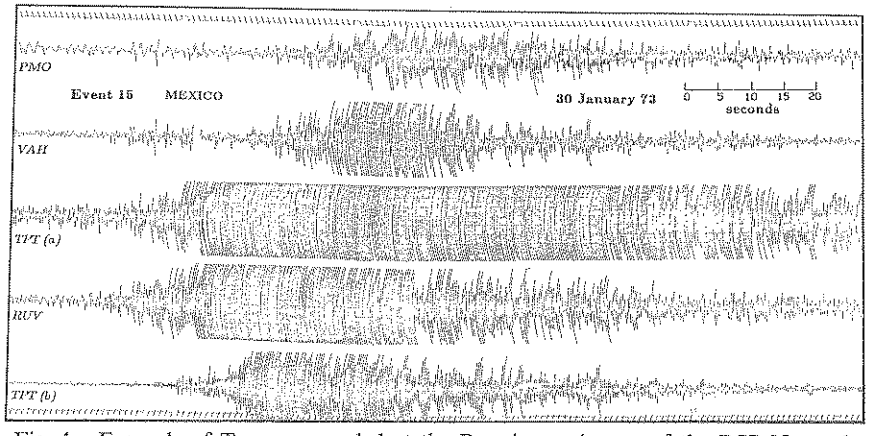

Fig. 4. Example of T wave recorded at the Rangiroa subarray of the RSP Network, for a Mexican event. See layout of stations on Fig. 1. Note that strong saturation of channel (a) (magnification 110,000 at 1 Hz) at Tiputa (TPT) on the northern shore, would lead to overestimating the duration of the maximum of the T wave. On the other hand, channel (b) (magnification 13,750 at 1 Hz) or channel (a) at Vaihoa (VAH) on the South coast, show compatible results.

of generation of the T wave may be very complex, due to extensive rupture at the source, near a strongly heterogeneous slope, leading to multipathing and to the development of a long coda. For this reason, we use different methods to measure duration, and consider different datasets, using differing magnitude scales and ranges.

3.1 Lower magnitudes; $\log_{10} \Theta$ vs. m_b

Our first dataset consists of T waves from 375 earthquakes of magnitudes

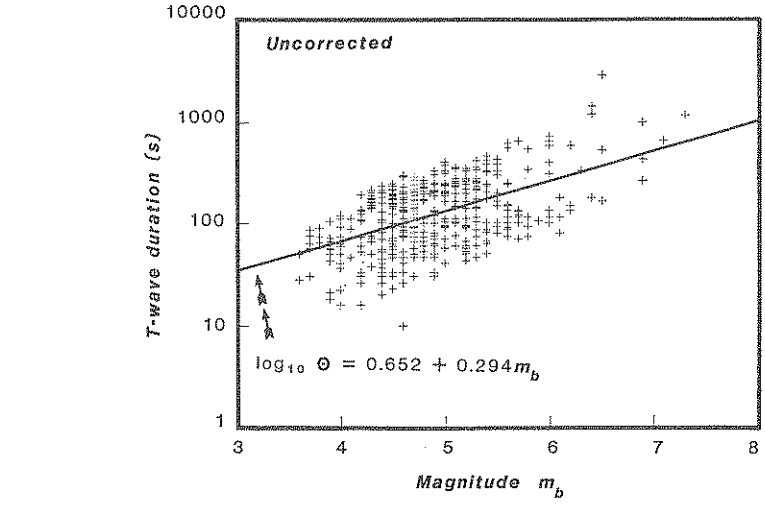

(a)

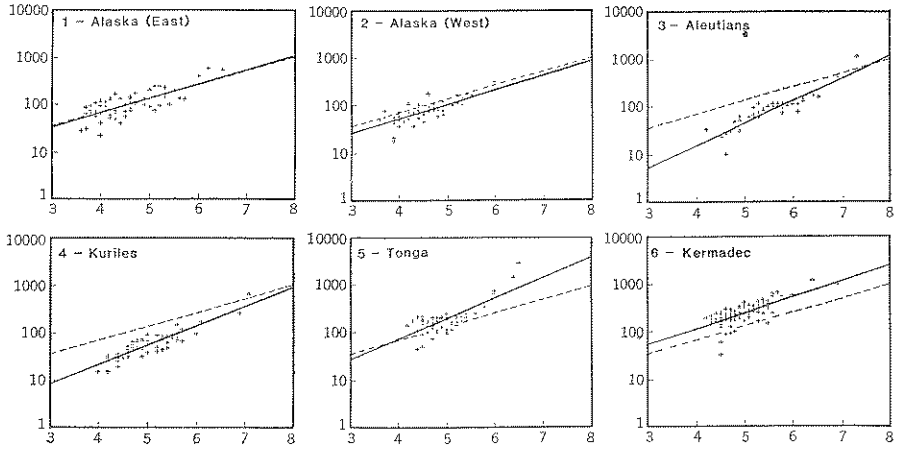

(b)

Fig. 5. (a) Duration of T waves as a function of body-wave magnitude m_b, for 375 Pacific earthquakes recorded in Polynesia. The straight line is a simple least-squares regression of the data. (b) Same as (a) for six representative data subsets, regionalized according to epicentral area. In each frame the full line is a regression to the regional data, and the dashed line is the full regression from (a). Note substantial offsets, with durations systematically longer from Tonga and Kermadec, and shorter from Aleutians and Kuriles. These subsets are used to define regional corrections.

Fig. 6. (a) Same as Fig. 5, after using regional corrections. Note the trend of Θ to grow faster at larger magnitudes, suggesting saturation of m_b. (b) Same as (a), after truncation of the dataset for $m_b<6$. Note excellent match of the experimental slope with the value predicted by Eq. (9c). (c) Same as (a), after truncation of the dataset for $m_b>5.5$. Note excellent match of the experimental slope with the value predicted by Eq. (9b).

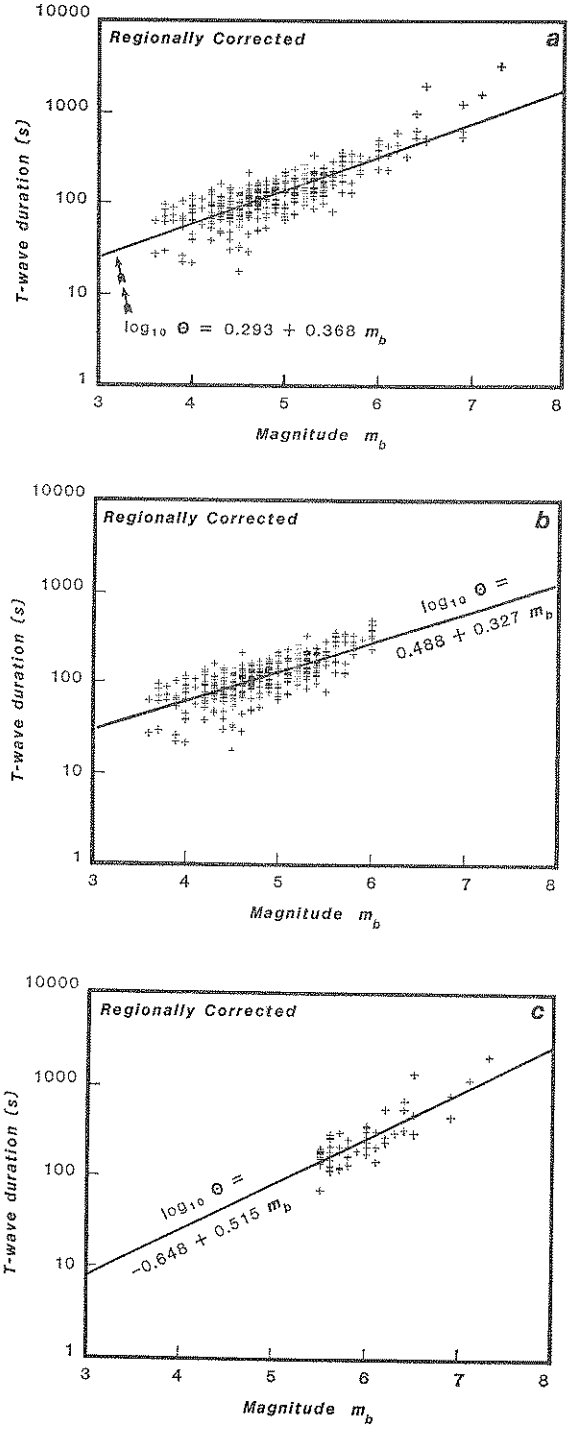
Regionally Corrected
a
T-wave duration (s)
10000
1000
100
10
1
3
4
5
6
7
8
Magnitude m_b
$\log_{10} \Theta = 0.293 + 0.368\ m_b$
Regionally Corrected
b
$\log_{10} \Theta =$
$0.488 + 0.327\ m_b$
Regionally Corrected
c
$\log_{10} \Theta =$
$-0.648 + 0.515\ m_b$

Fig. 6

m_b=3.6–7.3, located in 6 circum-Pacific regions, and recorded at stations of the RSP Network (TALANDIER, 1972). For these records, at relatively low magnitudes, Θ is measured as the duration of the T wave train emerging from background noise. Magnitudes are mostly reported m_b, with a potential problem as to the exact period at which these measurements were taken.

Figure 5 shows a plot of Θ as a function of magnitude for the whole dataset, as well as for selected epicentral regions. Significant results from Fig. 5 are: (i) the generally good agreement of the experimental slope of $\log_{10}\Theta$ vs. m_b with values intermediate between 0.3 and 0.5; (ii) the tendency for Θ to grow faster at larger magnitudes; and (iii) the existence of a significant regional offset in duration. In particular, Regions 5 (Tonga) and 6 (Kermadec) have T waves lasting on the average 5–7 times longer than other regions. Experiments with large explosive sources have shown that the amplitude of T waves decays with distance as $\Delta^{-3/2}$ (NORTHROP, 1968). Thus for the short distances between Polynesia and Tonga-Kermadec, the measured duration of the T wave train will be enhanced by amplification of its amplitude above noise level. In order to alleviate this difficulty, we define regional corrections for $\log_{10}\Theta$ from the 6 individual regressions for each epicentral region; these corrections are calculated as the average, for a given epicentral area, of the residual of $\log_{10}\Theta$ with respect to the linear regression for the whole dataset. (This procedure is similar to the definition of travel-time station corrections for use in relocation programs.) After applying these corrections, the total dataset appears much more homogeneous (Fig. 6(a)), and still exhibits the two characteristics (i) and (ii). In order to study the deviation of Θ at larger magnitudes, we split the dataset into $m_b<6$ and $m_b>5.5$. Figures 6(b) and 6(c) clearly show the difference in behavior, with regression slopes of respectively 0.33 and 0.51; these numbers are in excellent agreement with the theoretical values (1/3 and 1/2; see Eqs. (9)). One slight problem, however, is the range of magnitude at which this change takes place. Equations (9) predict a value of m_b=4.2, rather than m_b=5.5. This discrepancy may be due to the fact that values of m_b for large earthquakes are taken at periods significantly longer than the theoretical 1 s. This point was also noted by GELLER (1976).

3.2 Intermediate magnitudes; $\log_{10}\Theta$ vs. M_s

Our dataset for earthquakes of intermediate magnitudes consists of T wave records at stations of the RSP Network, from 110 events with magnitudes M_s= 6.0–8.5. For these events, the total duration of the T wave can reach several minutes, but its amplitude usually fluctuates significantly. This generally reflects the enhanced complexity of both the earthquake mechanism and the T wave generation process. For this reason, we characterize T-wave duration at intermediate magnitudes with two measurements, the total duration Θ_{tot} and the duration Θ_{sat} of saturation (40 mm peak-to-peak) of the T wave train on the standard short-period channel in Polynesia (with a gain of 100,000 at 1 Hz). Least-square regressions for the corresponding datasets yielded the following relations: $\log_{10}\Theta_{tot}$

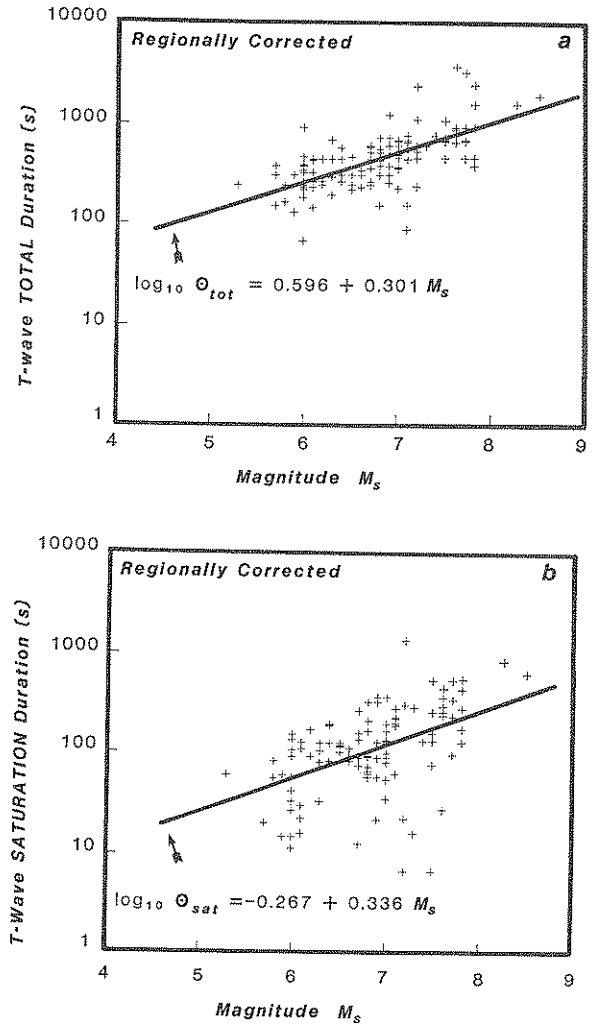

Fig. 7. T-wave duration Θ_{tot} and Θ_{sat} as a function of M_s for a set of 110 large earthquakes in the Pacific recorded at Polynesian stations. These durations have been corrected regionally. Note excellent agreement of the experimental slopes with the values predicted from Eq. (8c).

$=1.251+0.201M_s$ and $\log_{10}\Theta_{sat}=0.561+0.215M_s$. For those regions (Tonga, Aleutian, Kuriles, etc. . . .) where a sufficiently large dataset was available, we computed regional corrections, equal to the averaged residual between the observed $\log_{10}\Theta$ and that predicted from the global regression. We then ran a second set of least-squares regressions with the data so corrected, and obtained $\log_{10}\Theta_{tot}=0.596+0.301M_s$, and $\log_{10}\Theta_{sat}=-0.267+0.336M_s$. These results, shown in Figs. 7(a) and 7(b) are in excellent agreement with the theoretical slope

of 1/3 predicted from Section 2, especially given the uncertainties on the regressed slope itself (respectively ± 0.032 and ± 0.060).

3.3 *Truly large earthquakes; $\log_{10}\Theta$ vs. M_o (or M_w)*

3.3.1 *Dataset*

Table 1 lists 25 truly large earthquakes, all of which have moments of at least 10^{27} dyn-cm ($M_w > 7.2$). Because some of these events predate development of the RSP Network in French Polynesia, we also used T wave records at stations of the Hawaii Volcano Observatory Network (see KLEIN and KOYANAGI (1980) for details on its instrumentation). It was attempted to recover records of as

Table 1. Dataset of truly large earthquakes used in this study.

Number	Name or region	Date	Epicenter		Moment (10^{27} dyn-cm)	Fault length (km)	Reference (*)
			°N	°E			
1	Aleutian	9 Mar. 57	51.3	−175.8	600		a
2	Alaska	10 Jul. 58	58.3	−136.5	29	325	a, b
3	Kuriles	6 Nov. 58	44.4	148.6	40		a
4	Chile	22 May 60	−38.2	− 72.6	2,000	800	c
5	Kuriles	13 Oct. 63	44.9	149.6	70	250	d
6	Alaska	28 Mar. 64	61.1	−147.5	800	600	e
7	Rat Island	4 Feb. 65	51.3	178.5	140	500	f
8	Peru	17 Oct. 66	−10.7	− 78.6	20	80	g
9	Taltal	28 Dec. 66	−25.5	− 70.7	4	80	h
10	Tokachi-Oki	16 May 68	40.8	143.2	28	150	i
11	Kuriles	11 Aug. 69	43.4	147.8	22	200	j
12	Solomon Is.	14 Jul. 71	− 5.5	153.9	13		k
13	Kamchatka	15 Dec. 71	56.0	163.2	6		k
14	Alaska	30 Jul. 72	56.8	−135.9	7		k
15	Mexico	30 Jan. 73	18.5	−102.9	3		a
16	Nemuro-Oki	17 Jun. 73	43.1	145.7	7	60	l
17	Peru	3 Oct. 74	−12.2	− 77.6	18		a
18	Kalapana	29 Nov. 75	19.5	−155.1	1.2	30	m
19	Tonga	22 Jun. 77	−22.9	−175.7	20		n, o
20	Oaxaca	29 Nov. 78	15.8	− 96.8	3.5	85	p
21	Petatlán	14 Mar. 79	17.8	−101.3	2.7		o, q
22	Alaska	28 Feb. 79	60.7	−141.5	3	80	r
23	Sta. Cruz (foreshock)	8 Jul. 80	−12.4	166.4	2		s
24	Santa Cruz	17 Jul. 80	−12.5	165.9	8		s
25	Eureka	8 Nov. 80	41.1	−124.2	1.1	75	t

* References: (a) KANAMORI (1977); (b) BEN-MENAHEM and TOKSÖZ (1963); (c) KANAMORI and CIPAR (1974); (d) KANAMORI (1970 a); (e) KANAMORI (1970 b); (f) WU and KANAMORI (1973); (g) ABE (1972); (h) DESCHAMPS *et al.* (1980); (i) KANAMORI (1971); (j) ABE (1973); (k) This Study; (l) SHIMAZAKI (1974); (m) FURUMOTO and KOVACH (1979); (n) TALANDIER and OKAL (1979); (o) SILVER and JORDAN (1982); (p) STEWART *et al.* (1981); (q) MEYER *et al.* (1980); (r) HASEGAWA *et al.* (1980); (s) KANAMORI and GIVEN (1982); (t) LAY *et al.* (1982).

many tsunamigenic events as possible; unfortunately, this was not possible for the 1946 Aleutian earthquake, whose gigantic tsunami destroyed the city of Hilo, despite a relatively low M_s=7.4.

Energy magnitudes M_w and some rupture characteristics for events listed in Table 1 were obtained mostly from available literature. In the case of Events 13 and 14, no individual study was available, and these earthquakes were investigated separately, using WWSSN records: body-wave data yielded focal solutions, shown on Fig. 8, and synthetic long-period surface waves (Fig. 9) were used to obtain M_w, following the procedure of KANAMORI (1970 a). Event 13 involves slightly oblique subduction in the Kamchatka area, and Event 14 pure strike-slip motion along the Fairweather fault in the Alaskan panhandle.

For these very large earthquakes, the process of generation of the T wave may be complex, due to multipathing of the rays near the source, and leads to the

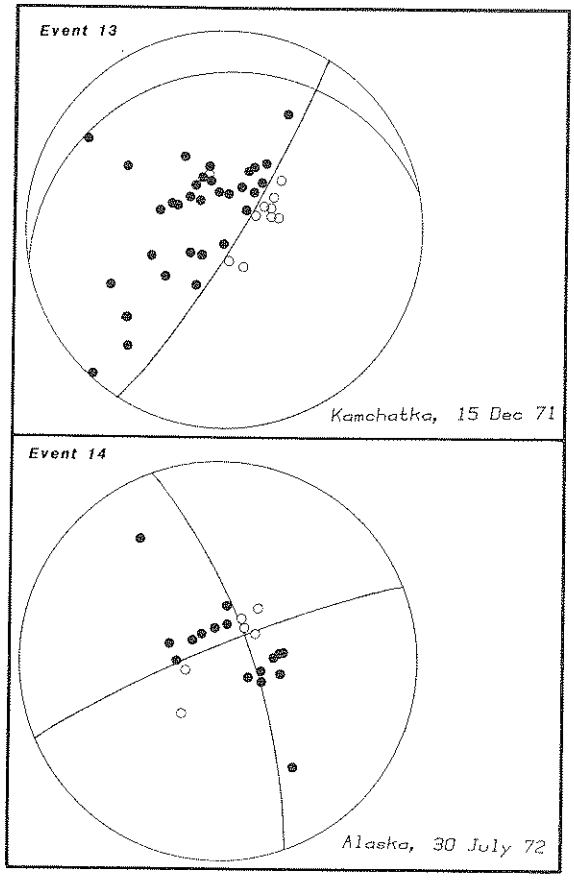

Fig. 8. Focal solutions obtained from P-wave first motions for Events 13 (Kamchatka, 1971) and 14 (Alaska, 1972). Stereographic projections of the lower focal hemispheres; full symbols are compressional arrivals, open ones dilatational.

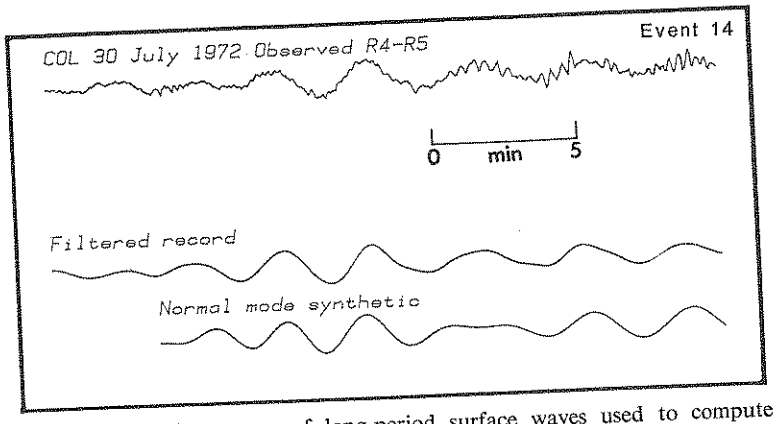

Fig. 9. Synthetic seismograms of long-period surface waves used to compute the seismic moment of Event 14. Top, observed record at College, Alaska of Rayleigh waves R_4 and R_5; Center, same record, filtered for periods greater than 45 s; Bottom, normal mode synthetics for the focal mechanism shown on Fig. 8. The seismic moment is retrieved through matching the amplitudes of the filtered and synthetic signals.

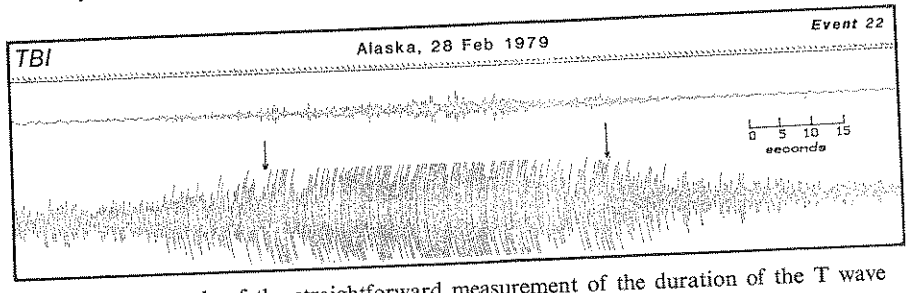

Fig. 10. Example of the straightforward measurement of the duration of the T wave at Tubuai (TBI) in the case of the 1979 Alaska event. Duration of the maximum in amplitude is defined by the two arrows.

development of a long coda, of decaying amplitude. Thus we use still another definition of the duration of the T wave as the duration Θ_{max} of sustained maximum recorded amplitude. Its measurement is straightforward in the case of a simple record such as that shown on Fig. 10, obtained for event 22 at Tubuai, French Polynesia (TBI), but a great deal of care has to be taken in the case of T waves of large amplitudes, which for truly large events may saturate considerably the dynamics of the more sensitive channels. The use of Θ_{sat} as the "duration" of the T wave train is no longer proper, since the saturation may mask the actual history of the amplitude of the wave, and thus lead to overestimating the length of the wave train. For example, in the case of Event 15 recorded at TPT (Fig. 4), channel (a), whose magnification is 115,000 at 1 Hz, saturates for about 80 s. In such cases, two methods can be used to obtain a more accurate measurement of the duration of the wave train: the use of lower gain channels, such as channel (b), at the same station, or measurements at a station further away from

the conversion slope, such as Vaihoa (VAH), where the transmitted seismic wave has been significantly attenuated during the propagation in the island. In principle, this last method could overestimate the duration, because of the possibility of

Table 2. T wave records used for truly large earthquakes.

Event number	Moment (10^{27} dyn-cm)	Station (†)	Measured duration (s)	Computed duration (s)	
				with directivity	without
1	600	HVO	120–180		145*
2	29	HVO	90	177	108
3	40	HVO	100		53
4	2,000	HIL	236	320	230
5	70	PAE	100	36	70
6	800	HIL	225	216	200
6	800	PPT	167	197	
7	140	PPT	173	405	165
8	20	RKT	100	76	27
9	4	HIL	50	5	27
10	28	PMO	124	133	43
11	22	PMO	50	30	57
11	22	PPN	37	30	57
12	13	HVO	70		
13	6	PPT	67		
14	7	TPT	128		33*
15	3	VAH	18		25*
15	3	MLO	47		25*
16	7	AFR	60	15	20
16	7	TPT	52	15	20
17	18	HVO	120		45*
17	18	RKT	84		45*
18	1.2	TPT	42		18
19	20	SPT	55		47*
19	20	PAE	60		47*
20	3.5	HVO	25	31	26
20	3.5	RUV	28	20	26
21	2.7	TPT	52	37	24*
22	3	TBI	56		27
22	3	TVO	68		27
23	2.1	SPT	63		33*
23	2.1	MLO	70		33*
24	8	SPT	136		60*
25	1.1	TPT	36		80
25	1.1	RUV	42		80

* Source duration estimated from scaling laws when no rupture parameters available.

† Hawaiian stations: HVO, Hawaiian Volcano Observatory; HIL, Hilo; MLO, Mauna Loa; SPT, South Point. Polynesian stations: PPT, Papeete, Tahiti; PAE, Paea, Tahiti; PPN, Papeeno, Tahiti; TVO, Taravao, Tahiti; AFR, Afareaitu, Moorea; TPT, Tiputa, Rangiroa; VAH, Vaihoa, Rangiroa; PMO, Pomariorio, Rangiroa; RUV, Rauvai, Rangiroa; TBI, Tubuai Island; RKT, Rikitea, Gambier.

multiple conversion sites (see discussion in Section 2.4). In practice, and given the small size of Polynesian atolls and islands, this effect is negligible, while the low values of Q characteristic of their shallow structures are enough to substantially reduce the recorded amplitudes. Comparison of these two methods in Fig. 4 reveals that the maximum of the amplitude of the T wave actually lasted for no more than 20 ± 5 s.

In any event, the precision which can be expected for a measurement of Θ_{max} is never better than ±5 s; it is more likely ±10 s.

3.3.2 Results

Table 2 presents a compilation of the records used for truly large events, and Fig. 11 explores the correlation between Θ_{max} and the energy magnitude M_w. In cases involving several records from the same event, an estimate of the systematic errors inherent in this method can be obtained. It is at once evident that a good correlation exists between Θ_{max} and M_w, especially for seismic moments greater than 2×10^{28} dyn-cm ($M_w\geq8.1$) and durations longer than 100 s. This correlation becomes less good for smaller events: in this case, the contribution of rupture length to the duration of the T wave train becomes less significant, relative to sources of errors, such as dispersion and multipathing.

This dataset satisfies Eq. (7) (modeled as a dashed line on Fig. 11) with a standard deviation of only $\sigma=0.49$, within the range of the uncertainty of the unknown constant C in Eq. (4). On the other hand, the dataset can be fit to a straight line in several ways. If we assume that the seismic moments are well known, and fit a formula of the type

$$\log_{10}\Theta=xM_w+y\pm\sigma\ , \tag{10}$$

we obtain $x=0.61$; $y=-3.06$; $\sigma=0.34$. By reversing the roles, assuming that Θ is well known, and fitting a formula of the form:

$$M_w=x'\log_{10}\Theta+y'\pm\sigma'\ , \tag{11}$$

we find $x'=2.75$; $y'=2.93$, corresponding to $x=0.37$; $y=-1.07$ in Eq. (10). Finally, the straight line minimizing the sum of distances

$$\alpha\log_{10}\Theta+\beta M_w-\gamma \tag{12}$$

(where $\alpha^2+\beta^2$ is constrained to 1) corresponds to $x=0.40$; $y=-1.32$ in Eq. (10). These various linear regressions of the dataset are shown as dash-dot lines on Fig. 11. Given the systematic errors discussed in Section 2, and the uncertainties in measuring Θ, this must be considered an excellent fit to Eq. (7), which justifies our approach.

Table 2 also presents an estimate of the effect of directivity on duration at the stations used. For this purpose, Eq. (2) was utilized, whenever rupture parameters could be retrieved from the literature. Such an estimate was not computed for rupture lengths L less than 80 km, since the corresponding contribution to the duration Θ is on the order of 30 s or less. As shown by the data in Table

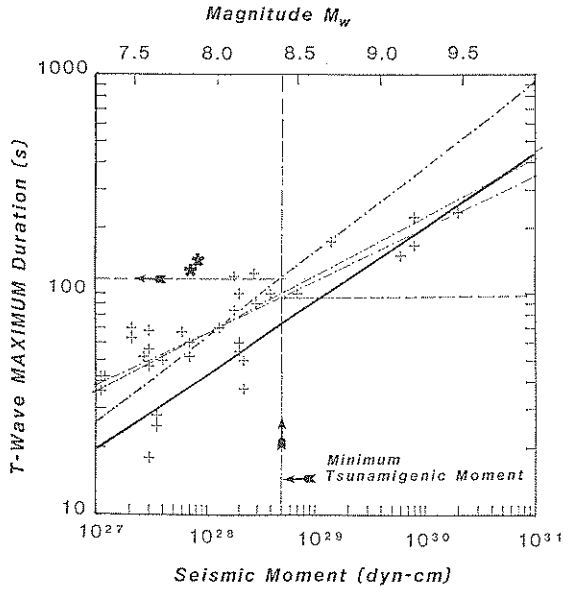

Fig. 11. Duration of T waves plotted in relation to seismic moment M_0 (lower scale), or equivalently energy magnitude M_w (upper scale). The oblique solid line is the theoretical relationship predicted by Eq. (4). The dash-dot lines are the various regressions of the data to a linear relation between M_w and $\log_{10} \Theta$ (see text for details). The vertical dash line (with vertical arrow), drawn at a moment of 5×10^{29} dyn-cm, represents the threshold of earthquakes potentially dangerous in terms of damaging tsunamis.

2, the adequacy of Eq. (2) is extremely variable: in some instances, such as the Alaskan earthquake of 1964, it gives excellent results, and correctly describes the difference in duration in Hawaii and Tahiti; this suggests that the conversion from seismic to acoustic energy took place regularly all along the rupture. In other cases such as the Rat Island earthquake of 1965, or the Kuriles earthquake of 1963, Eq. (2) yields durations either much shorter or much longer than actually observed, while putting $C=1$ in Eq. (4) gives a much better answer. In the general framework of Section 2.5, this simply means that the generation of T waves is probably concentrated at a favorable point along the slope, away from the epicenter and that Θ reflects only the duration of rupture of the source, rather than a difference in path for T waves from the individual sources.

4. *Discussion: Potential for Use in Tsunami Warning*

Our results clearly suggest that at least some information on the size of a truly major earthquake can be obtained from the duration of the T wave trains recorded at faraway stations. In this respect, and despite all the problems due to our incomplete knowledge of the conditions of generation of the T waves in the

vicinity of the parent earthquake, an excellent match is obtained with both the slope and baseline predicted by Eq. (7), derived from an extremely simple model of earthquake source and rupture. This indicates that for these very large earthquakes, the rupture time of the source is the major agent controlling the duration of maximum sustained amplitude observable on low-gain channels. When dealing with smaller earthquakes, this contribution decreases both in duration and amplitude, so that the duration of maximum amplitude can no longer be measured, and only the total duration Θ_{max} is accessible. The fact that the observed regression slopes still match their theoretical values indicates that rupture length is the only contributor to T wave duration which is sensitive to earthquake size, as opposed to other agents (such has multipathing due to seamount reflections).

From a practical point of view, the following numbers provide a rule of thumb for the scaling of seismic moments from T wave duration: if the duration of the maximum amplitude of the T waves is 80 s or less, the seismic moment is $\leq 10^{28}$ dyn-cm; if it lasts 150 s, the moment is 10^{29}, and more than 3 min, it approaches 10^{30}. These numbers must however be taken with large uncertainties: in particular, considerable scatter exists at the lower end of the moment scale.

In discussing the potential of this method in tsunami warning procedures, it must be kept in mind that tsunami danger exists Pacific-wide only for truly gigantic earthquakes, with moments larger than about 5×10^{28} dyn-cm, corresponding to a high-sea tsunami amplitude of 20 cm or more, assuming a focal mechanism favorable to tsunami excitation (WARD, 1980). Only then can converted waves at the shorelines be amplified to destructive levels at teleseismic distances. This line separating "moderate" from "potentially tsunamigenic" earthquakes is drawn as the vertical dash line on Fig. 11; depending on which regression is chosen, the corresponding T-wave duration falls 95 and 130 s. These lines are drawn on Fig. 11 as the two horizontal dash segments. They represent the T-wave duration threshold for the generation of a tsunami. We use two discontinuous segments, rather than a single line to emphasize the deviation between the various regressions. Events plotted in the lower right quadrant delimited on Fig. 11 by the dash lines could be undetected tsunamigenic earthquakes; events belonging to the upper left quadrant would be false alarms.

In this respect, no truly gigantic events in our catalogue (having generated Pacific-wide destructive tsunamis) had T wave trains with maximum amplitudes lasting less than 2 min. However, we must discuss more in detail the case of the grossly over-estimated events, which could have led to "false alarms" (Events 14 and 24; shown as asterisks on Fig. 11).

Event 14, along the Fairweather fault of Alaska, was characterized by a multiple rupture, as clearly shown by the complexity of its long-period body waves: Fig. 12(a) shows the PKP arrivals at South Pole (SPA), a station 146.7° away, where the total duration of the PKP group should be minimal. Note the complexity of the wave train, lasting for up to two minutes after the first arrival; this behavior is also apparent in the phase SKP, and is compatible with observed dura-

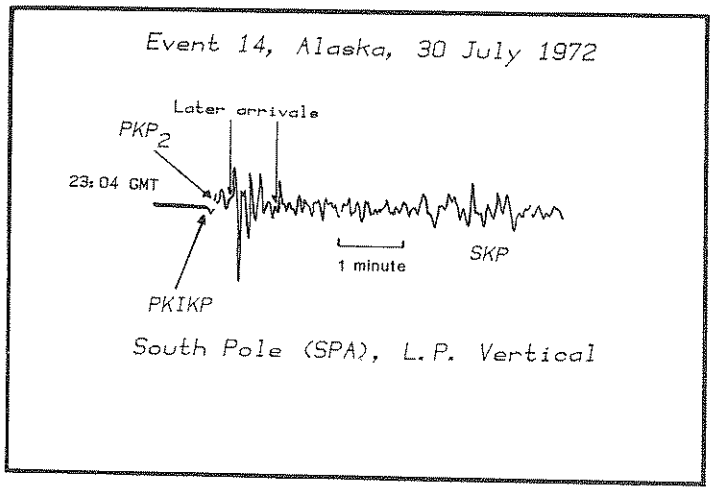

(a)

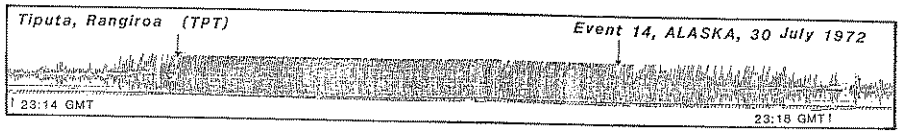

(b)

Fig. 12. (a) Long-period PKP and SKP waves observed at South Pole following the 1972 Fairweather Fault, Alaska, earthquake. Arrows denote various phases, and additional arrivals corresponding to subsequent sources. This record demonstrates the complexity of the event. (b) T wave record of the Fairweather event of 1972 at TPT. This record is on the low-gain channel (13,750 at 1 Hz). Note exceptional amplitude of T waves, and duration (arrows) of more than 2 min.

tion of the T waves at TPT (see Fig. 12(b)). The fact that its seismic moment computed from surface waves falls short of the estimate from duration may be caused by its multiplicity: In the case of a geometry with a particularly high value for the constant C of Eq. (4), several relatively small events separated by a time lapse comparable to the duration of the T waves at a given station will give the wave train a prolonged character, while not contributing to the ultra-low frequency surface waves as efficiently as would a single rupture, sustained in time. It is however worth noting that while no Pacific-wide tsunami was reported following this earthquake, it did generate seiches in swimming pools in Seattle, 1,300 km away.

No rupture mechanism is available for Event 24 (Santa Cruz mainshock, 17 July 1980). The moment values used in the present analysis were taken from the results of KANAMORI and GIVEN (1982). It is worth noting that this is one of the few events for which these authors used a full moment tensor inversion, without constraining the dip-slip components to zero. However, a substantial second double-couple (19%) is required by the inversion. A complex source involving

several sub-events with different focal mechanisms in a sense comparable to the case of Event 14, could explain this result.

This third, "great earthquake" dataset is not large enough to allow the statistical computation of regional corrections, similar to those computed for the first two datasets. However, if we applied the corrections found in Section 3.2 for Θ_{sat} values, which among other things reflect the relative proximity of the Southwest Pacific subduction zones to Tahiti, we would reduce the discrepancy between observed and computed durations for the Santa Cruz event, which would then not qualify as a false alarm.

In conclusion, our very simple theoretical models for the origin of the duration of T waves are upheld, at various magnitude ranges, for records gathered over more than 20 years' time in Polynesia. In particular, for very large events, T-wave duration can be used to compute in real time an estimate of the seismic moments with an uncertainty estimated to be within a factor of 3; this compares well with present-day accuracy for real-time moment solutions, and thus this method continues to be of great interest for tsunami warning.

We are grateful to the Director and Staff of Hawaii Volcano Observatory for their hospitality and numerous discussions concerning the HVO network. We thank Yves Cansi for fruitful discussions, and Seth Stein for a critical review. This study was supported by Commissariat à l'Energie Atomique, NOAA under Contract N-80-RAD-00014, the Office of Naval Research under Contracts N00014-C-79-0292 and N00014-84-C-0616, and the National Science Foundation, under Grant EAR-84-05040.

REFERENCES

ABE, K., Mechanism and tectonic implications of the 1966 and 1970 Peru earthquakes, *Phys. Earth Planet. Inter.*, **5**, 367–379, 1972.

ABE, K., Tsunami and mechanisms of great earthquakes, *Phys. Earth Planet. Inter.*, **7**, 143–153, 1973.

ABE, K., Size of great earthquakes of 1837–1974 inferred from tsunami data, *J. Geophys. Res.*, **84**, 1561–1568, 1979.

AGNEW, D., J. BERGER, R. P. BULAND, W. FARRELL, and J. F. GILBERT, International deployment of accelerometers: A network for very long period seismology, *EOS, Trans. Am. Geophys. Un.*, **57**, 180–188, 1976.

BEN-MENAHEM, A. and M. ROSENMAN, Amplitude patterns of tsunami waves from submarine earthquakes, *J. Geophys. Res.*, **77**, 3097–3128, 1972.

BEN-MENAHEM, A. and M. N. TOKSÖZ, Source mechanism from spectra of long-period seismic surface waves. 3. The Alaska earthquake of July 10, 1958, *Bull. Seismol. Soc. Am.*, **53**, 905–919, 1963.

CANSI, Y., Etudes expérimentales d'ondes T, *Thèse de 3ème cycle*, Orsay, 101 pp., 1981.

CANSI, Y., Interprétation d'un train d'ondes T généré par une explosion sous-marine et détecté par un réseau de seismographes, *Int. Rep.*, Commissariat à l'Energie Atomique, Paris, 52 pp., 1982.

CANSI, Y. and N. BETHOUX, T waves with long inland paths: Synthetic seismograms, *J. Geophys. Res.*, **90**, 5459–5465, 1985.

DESCHAMPS, A., H. LYON-CAEN, and R. MADARIAGA, Etude du tremblement de terre de Taltal (Chili) à partir des ondes sismiques de longue période, *Ann. Géophys.*, **36**, 179–190, 1980.

EATON, J. P., D. H. RICHTER, and W. U. AULT, The tsunami of May 23, 1960 on the island of Hawaii, *Bull. Seismol. Soc. Am.*, **51**, 135–157, 1961.

EWING, M., I. TOLSTOY, and F. PRESS, Proposed use of the T phase in tsunami warning systems, *Bull. Seismol. Soc. Am.*, **40**, 53–58, 1950.

FUKAO, Y., Tsunami earthquakes and subduction processes near deep-sea trenches, *J. Geophys. Res.*, **84**, 2303–2314, 1979.

FURUMOTO, A. S. and R. L. KOVACH, The Kalapana earthquake of November 29, 1975: An intraplate earthquake and its relation to geothermal processes, *Phys. Earth Planet. Inter.*, **18**, 197–208, 1979.

GELLER, R. J., Scaling relations for earthquake source parameters and magnitudes, *Bull. Seismol. Soc. Am.*, **66**, 1501–1523, 1976.

HASEGAWA, H. S., J. C. LAHR, and C. D. STEPHENS, Fault parameters of the St. Elias, Alaska, earthquake of February 28, 1979, *Bull. Seismol. Soc. Am.*, **70**, 1651–1660, 1980.

HERRMANN, R. B., The use of duration as a measure of seismic moment and magnitude, *Bull. Seismol. Soc. Am.*, **65**, 899–913, 1975.

IIDA, K., The generation of tsunamis and the focal mechanism of earthquakes, in *Tsunamis in the Pacific Ocean*, ed. W. M. Adams, pp. 3–18, East-West Press, Honolulu, 1970.

JOHNSON, R. H. and R. A. NORRIS, Geographic variation of SOFAR speed and axis depth in the Pacific Ocean, *J. Geophys. Res.*, **73**, 4695–4700, 1968.

KANAMORI, H., Synthesis of long-period surface waves and its application to earthquake source studies—Kurile Islands earthquake of October 13, 1963, *J. Geophys. Res.*, **75**, 5011–5027, 1970 a.

KANAMORI, H., The Alaska earthquake of 1964: Radiation of long-period surface waves and source mechanism, *J. Geophys. Res.*, **75**, 5029–5040, 1970 b.

KANAMORI, H., Focal mechanism of the Tokachi-Oki earthquake of May 16, 1968: Contortion of the lithosphere at a junction of two trenches, *Tectonophysics*, **12**, 1–13, 1971.

KANAMORI, H., Mechanism of tsunami earthquakes, *Phys. Earth Planet. Inter.*, **6**, 346–359, 1972.

KANAMORI, H. The energy release in great earthquakes, *J. Geophys. Res.*, **82**, 2981–2987, 1977.

KANAMORI, H. and D. L. ANDERSON, Theoretical basis of some empirical relations in seismology, *Bull. Seismol. Soc. Am.*, **65**, 1073–1095, 1975.

KANAMORI, H. and J. J. CIPAR, Focal process of the great Chilean earthquake of May 22, 1960, *Phys. Earth Planet. Inter.*, **9**, 128–136, 1974.

KANAMORI, H. and J. W. GIVEN, Use of long-period surface waves for rapid determination of earthquake source parameters. 2. Preliminary determination of source mechanisms of large earthquakes ($M_s \geq 6.5$) in 1980, *Phys. Earth Planet. Inter.*, **30**, 260–268, 1982.

KANAMORI, H. and J. W. GIVEN, Use of long-period seismic waves for rapid evaluation of tsunami potential of large earthquakes, in *Tsunamis—Their Science and Engineering*, ed. K. Iida and T. Iwasaki, pp. 37–49, TERRAPUB, Tokyo, 1983.

KLEIN, F. W. and R. Y. KOYANAGI, Hawaiian Volcano Observatory seismic network history 1950–79, *U.S. Geol. Surv. Open File Rep.*, **80–302**, 1980.

LAY, T. and H. KANAMORI, An asperity model of large earthquake sequences, in *Earthquake Prediction, an International Review*, ed. D. W. Simpson and P. G. Richards, Maurice Ewing Ser., Vol. 4, pp. 579–592, Am. Geophys. Un., Washington, D. C., 1981.

LAY, T., J. W. GIVEN, and H. KANAMORI, Long-period mechanism of the 8 November 1980 Eureka, California earthquake, *Bull. Seismol. Soc. Am.*, **72**, 439–456, 1982.

MEYER, R. P., W. D. PENNINGTON, L. A. POWELL, W. L. UNGER, M. GUZMÁN, J. HAVSKOV, S. K. SINGH, C. VALDÉS, and J. YAMAMOTO, A first report on the Petatlán, Guerrero, Mexico earthquake of 14 March 1979, *Geophys. Res. Lett.*, **7**, 97–100, 1980.

NORTHROP, J., Submarine topographic echoes from chase V, *J. Geophys. Res.*, **73**, 3909–3915, 1968.

NORTHROP, J., T phases from the Hawaiian earthquake of April 26, 1973, *J. Geophys. Res.*, **79**, 5478–5481, 1974.

PORTER, R. P., Dispersion of axial SOFAR propagation in the western Mediterranean, *J. Acoust. Soc. Am.*, **53**, 181–191, 1973.

SHIMAZAKI, K., Nemuro-Oki earthquake of June 17, 1973: A lithospheric rebound at the upper half of the interface, *Phys. Earth Planet. Inter.*, **9**, 314–327, 1974.

SILVER, P. G. and T. H. JORDAN, Optimal estimation of scalar seismic moment, *Geophys. J. R. Astron. Soc.*, **70**, 755–787, 1982.

SOMMERFELD, A., *Optics, Lectures on Theoretical Physics*, Vol. 4, Academic Press, New York, 1964.

STEWART, G. S., E. P. CHAEL, and K. C. MCNALLY, The November 29, 1978, Oaxaca, Mexico earthquake: A large simple event, *J. Geophys. Res.*, **86**, 5053–5060, 1981.

SUTEAU, A. M. and J. H. WHITCOMB, A local earthquake coda magnitude and its relation to duration, moment M_0, and local Richter magnitude M_L, *Bull. Seismol. Soc. Am.*, **69**, 353–368, 1979.

TALANDIER, J., Contribution à la prévision des tsunamis, *C.R. Acad. Sci. Paris, Sér. B*, **263**, 940–942, 1966.

TALANDIER, J., Etude et prévision des tsunamis en Polynésie Française, *Thèse d'Université*, Paris, 128 pp., 1972.

TALANDIER, J. and E. A. OKAL, Human perception of T waves: The June 22, 1977 Tonga earthquake felt on Tahiti, *Bull. Seismol. Soc. Am.*, **69**, 1475–1486, 1979.

WARD, S. N., Relationship of tsunami generation and an earthquake source, *J. Phys. Earth*, **28**, 441–474, 1980.

WATANABE, H., Statistical study of tsunami sources and tsunamigenic earthquakes occurring in and near Japan, in *Tsunamis in the Pacific Ocean*, ed. W. M. Adams, pp. 99–118, East-West Press, Honolulu, 1970.

WU, F. and H. KANAMORI, Source mechanism of February 4, 1965, Rat Island Earthquake, *J. Geophys. Res.*, **78**, 6082–6092, 1973.